NeuroImage: Clinical 30 (2021) 102624

Contents lists available at ScienceDirect

NeuroImage: Clinical

journal homepage: www.elsevier.com/locate/ynicl

Cortical volume reductions as a sign of secondary cerebral and cerebellar impairment in patients with degenerative cervical myelopathy

Kerstin Jütten [a], Verena Mainz [b], Gerrit Alexander Schubert [a], Robin Fabian Gohmann [c,d], Tobias Schmidt [a], Hani Ridwan [e], Hans Clusmann [a], Christian Andreas Mueller [a], Christian Blume [a,*]

[a] Department of Neurosurgery, RWTH Aachen University, Pauwelsstraße 30, 52074 Aachen, Germany
[b] Institute of Medical Psychology and Medical Sociology, RWTH Aachen University, Pauwelsstraße 19, 52074 Aachen, Germany
[c] Department of Diagnostic and Interventional Radiology, Heart Center Leipzig, Strümpelstraße 39, 04289 Leipzig, Germany
[d] Medical Faculty, University of Leipzig, Liebigstraße 27, 04103 Leipzig, Germany
[e] Department of Diagnostic and Interventional Neuroradiology, RWTH Aachen University, Pauwelsstraße 30, 52074 Aachen, Germany

ARTICLE INFO

Keywords:
Degenerative cervical myelopathy
Gray matter volume alterations
Voxel-based morphometry

ABSTRACT

This study investigated supra- and infratentorial structural gray and white matter (GM, WM) alterations in patients with degenerative cervical myelopathy (DCM) as an indicator of secondary harm due to chronic cervical cord compression and micro trauma. With MRI-based anatomical assessment and subsequent voxel-based morphometry analyses, pre- and postoperative volume alterations in the primary motor cortex (MI), the primary somatosensory cortex (SI), the supplementary motor area (SMA), and the cerebellum were analyzed in 43 DCM patients and 20 controls. We assessed disease-related symptom severity by the modified Japanese Orthopaedic Association scale (mJOA). The study also explored symptom severity-based brain volume alterations as well as their association with clinical status. Patients had lower mJOA scores ($p = .000$) and lower GM volume than controls in SI ($p = .016$) and cerebellar regions ($p = .001$). Symptom severity-based subgroup analyses revealed volume reductions in almost all investigated GM ROIs (MI: $p = .001$; CB: $p = .040$; SMA: $p = .007$) in patients with severe clinical symptoms as well as atrophy already present in patients with moderate symptom severity. Clinical symptoms in DCM were associated with cortical and cerebellar volume reduction. GM volume alterations may serve as an indicator of both disease severity and ongoing disease progression in DCM, and should be considered in further patient care and treatment monitoring.

1. Introduction

The most frequent chronic impairment of the spinal cord is caused by degenerative cervical myelopathy (DCM) (Shamji et al., 2013). As the global population ages, incidences of degenerative cervical spine disease are expected to increase significantly (Fehlings et al., 2015). The consequences of untreated DCM can be devastating for patients, possibly resulting in severe spinal cord injury and tetra paresis (Fehlings et al., 2013). Up to now, surgical decompression is the only known and effective treatment option for patients with DCM. After surgery, approximately 50% of the patients are able to improve their clinical-neurological status (Tetreault et al., 2015). However, even after anatomically successful surgery, some patients experience no improvement or even a deterioration in their clinical status (Fehlings et al., 2012).

As a unique entity, DCM is caused by continuous compression and repetitive micro-trauma of the spinal cord (Shamji et al., 2013). Apart from such mechanical injuries to the spinal cord, pathomechanisms of additional, secondary harm have attracted much scientific attention in recent years. Endogenous immune-mediated reactions to inflammation and angiogenesis in the spinal cord have been described (Karadimas et al., 2013a, 2015b, 2013c; Blume et al., 2021), all well as disruption of the blood spinal cord barrier (BSCB) (Karadimas et al., 2013; Blume et al., 2020; Fehlings et al., 1989). As opposed to more complex radiological markers for microstructural and metabolic changes, pathological T2w signal increase of the spinal cord and the degree of stenosis are only weak indicators of neuronal impairment, and do not correlate well with disease severity or duration (Ellingson et al., 2015).

* Corresponding author.
E-mail address: cblume@ukaachen.de (C. Blume).

https://doi.org/10.1016/j.nicl.2021.102624
Received 5 October 2020; Received in revised form 4 March 2021; Accepted 5 March 2021
Available online 13 March 2021
2213-1582/© 2021 Published by Elsevier Inc. This is an open access article under the CC BY-NC-ND license (http://creativecommons.org/licenses/by-nc-nd/4.0/).

Different studies have evaluated the impact of DCM in certain brain areas. Application of further imaging techniques such as magnetic resonance spectroscopy have elucidated severe derangement of cellular functions, changes of important neuro-metabolites and loss of neuronal integrity in cerebral and cerebellar areas during DCM pathogenesis (Aleksanderek et al., 2017; Wen et al., 2014; Kowalczyk et al., 2012; Craciunas et al., 2017). Thus, the effect of chronic compression and repetitive traumas of the spinal cord is not limited to the anatomical area where the main impairment occurs. Clinical symptoms in DCM seem to be the result of both the impairment due to the spinal cord injury and cortical/cerebellar abnormalities (Dong et al., 2008; Duggal et al., 2010; Tan et al., 2015). Recent studies detected brain volumetric changes in DCM patients. Significant atrophy of the sensorimotor cortices has been implicated as secondary harm to cortical structures in association with chronic compression of the spinal cord (Wang et al., 2018; Bernabéu-Sanz et al., 2020). More specifically, the primary motor and primary somatosensory cortex (MI and SI), the supplementary motor area (SMA) as well as subcortical structures have been associated with volumetric changes (atrophy) in case of spinal cord injury (Wang et al., 2018; Freund et al., 2011; Hou et al., 2014). Similar effects have been observed in gray and white matter (GM and WM) of cerebellar areas (Dong et al., 2008; Duggal et al., 2010; Tan et al., 2015).

The aim of this study was to explore disease-related brain volumetric changes and plasticity in DCM patients using advanced anatomical MRI techniques. Mirrored by the clinical symptoms of DCM, specific GM and WM cerebral regions in MI and SI, cerebellar and upper cervical spinal cord areas were investigated for volumetric deviations and compared to controls. Furthermore, we explored longitudinal volumetric changes during disease progression, and examined the association of clinical parameters with brain volumetric changes. We hypothesized that patients would show volume reductions in the brain regions examined, and assumed that surgery would pause further disease-related changes. In addition, we hypothesized that initial structural parameters and alterations of the brain would correlate with the clinical status in DCM.

2. Materials and methods

2.1. Participants

43 treatment-naíve patients with DCM (mean age: 61 ± 11 years, 27 males) and 20 healthy controls (HC, mean age: 64 ± 6 years, 11 males) were enrolled in the study at a single university hospital center. All patients underwent surgery, with 21 included for follow-up examination after three months. Participants were excluded if they showed neurological disorders other than DCM (e.g. neurodegenerative diseases), history of cerebral stroke, cerebral hemorrhage, central nervous infections or spinal trauma. All participants gave written informed consent. The study was approved by the local ethics committee (EK 164/13) and conducted in accordance with the standards of Good Clinical Practice and the Declaration of Helsinki.

2.2. Clinical assessment

All participants underwent a standardized clinical examination, comprising the assessment of demographic information and neurological status, as evaluated by the modified Japanese Orthopaedic Association scale (mJOA) and the Neck Disability Index (NDI).

The mJOA is used to evaluate neurological function in patients with DCM (Yonenobu et al., 2001). A score of 18 reflects no neurological deficits, whereas a lower score indicates some degree of disability and functional impairment. To analyze clinical subgroups based on the severity of symptoms, scores were subdivided according to (Tetreault et al., 2017) into none-mild (mJOA 18–15), moderate (mJOA 12–14) and severe (mJOA 0–11) symptoms, resulting in clinical subgroups of n = 27, n = 12, and n = 24, respectively.

The NDI assesses the effect of neck pain on the ability to manage everyday life (Vernon and Mior, 1991). A low score indicates no (0–4), mild (5–14), moderate (15–24), severe (25–34) problems, whereas a score above 34 reflects the complete inability to manage the activities of everyday life.

2.3. MRI data acquisition

All participants underwent an MRI examination on a 3 T Siemens Prisma MRI scanner equipped with a standard 20-channel head coil. Patients' initial and follow-up acquisitions were performed directly prior to surgery as well as three months after surgery. The scanning protocol included a sagittal 3D T1 magnetization-prepared rapid acquisition gradient echo sequence, repetition time (TR) = 2.300 ms, echo time (TE) = 2.98 ms, 176 slices with a slice thickness of 1 mm, flip angle (FA) = 9°, field of view (FOV) = 256 mm, voxel size = 1 mm isotropic, and 256 × 256 matrix. To exclude HC with clinical inapparent cervical stenosis, a sagittal T2W images of the cervical spine was performed, TR = 4000 ms, TE = 111 ms, 17 slices with a slice thickness of 3 mm, FA = 160°, voxel size = 3 × 3 × 3.2 mm, and 512 × 384 matrix.

2.4. Preprocessing and structural analyses

Image preprocessing was carried out using the Computational Anatomy Toolbox (CAT12, http://www.neuro.uni-jena.de/cat/), which is SPM12-based (Friston et al., 2006) as implemented in Matlab 9.3. Applying the voxel-based morphometry procedure implemented in CAT12, individual structural images were first segmented into GM, WM and cerebro-spinal fluid. GM and WM volume of regions of interest (ROIs) were then extracted from the Jülich cytoarchitectonic atlas (Eickhoff et al., 2005), amended by the AAL atlas (Tzourio-Mazoyer et al., 2002), and included the primary motor cortex (MI, areas 4a, 4p), the primary somatosensory cortex (SI, areas 1, 2, 3a, 3b), the cerebellar hemispheres (areas IV, V, VI, VIIb, VIIIa, VIIIb, IX, X), and the supplementary motor area (SMA). Left- and right-hemispheric tissue volumes of selected ROIs were averaged. All included ROIs are displayed in Fig. 1.

Left- and right-hemispheric regions of interest (ROIs) are displayed, overlaid on a T1 standard brain template. They were extracted from the Jülich cytoarchitectonic atlas (Eickhoff et al., 2005) and amended by the AAL atlas (Tzourio-Mazoyer et al., 2002) and included the primary motor cortex (MI, areas 4a, 4p), the primary somatosensory cortex (SI, areas 1, 2, 3a, 3b), the cerebellar hemispheres (areas IV, V, VI, VIIb, VIIIa, VIIIb, IX, X), and the supplementary motor area (SMA), respectively.

Furthermore, the intracranial volume (ICV) was estimated as the sum of GM, WM and CSF and used to correct for inter-individual differences in brain size. Apart from ascertaining that no group differences existed in ICV (p = .100), we included additional cerebral "control" regions unlikely to be involved in disease-related changes in the analysis. Specifically, parts of the fusiform gyrus (areas FG1, FG2, FG3, and FG4) and the hippocampus (areas CA, DG, EC, HATA, Subc) were chosen from the Jülich cytoarchitectonic atlas and compared between patients and HC. To account for a possible upward progression of atrophy, volume of the mean upper cervical cord area was extracted (MUCCA, (Liu et al., 2016)) by applying a semi-automatically segmentation procedure using ITKsnap (Yushkevich et al., 2006). An overview of all methods applied can be found in Fig. 2.

The initial (i.e. prior to surgery) MRI examination was acquired from 43 patients (PAT) and 20 healthy controls (HC). 21 patients could be included in the post-operative follow-up examination three months later. Image (pre)processing included the normalization of subjects' 3D T1 images to a standard brain in MNI space, the segmentation into gray matter (GM), white matter (WM) and cerebrospinal fluid (CSF), and the volume extraction of atlas-based chosen regions of interest (ROI). Extracted ROI volumes were then analyzed applying multivariate analyses of covariance, comparing between groups as well as pre- (t_1) and

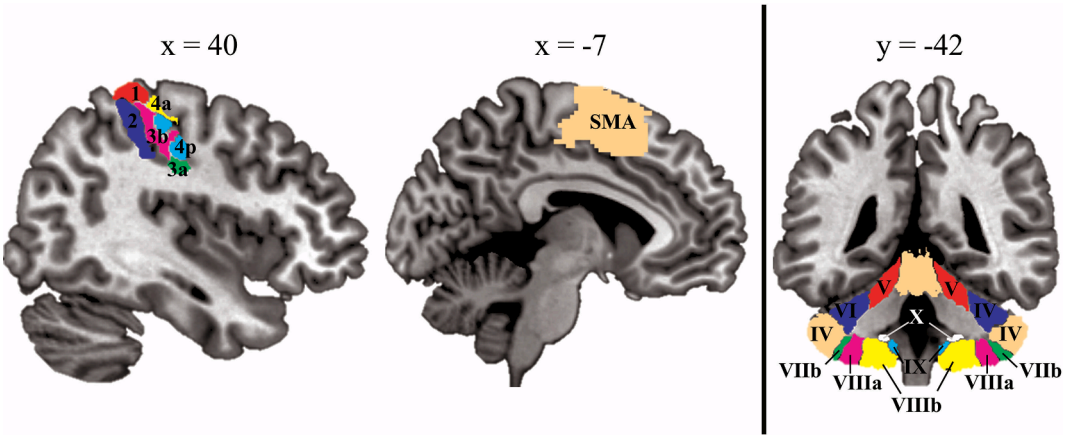

Fig. 1. Visualization of analyzed ROIs.

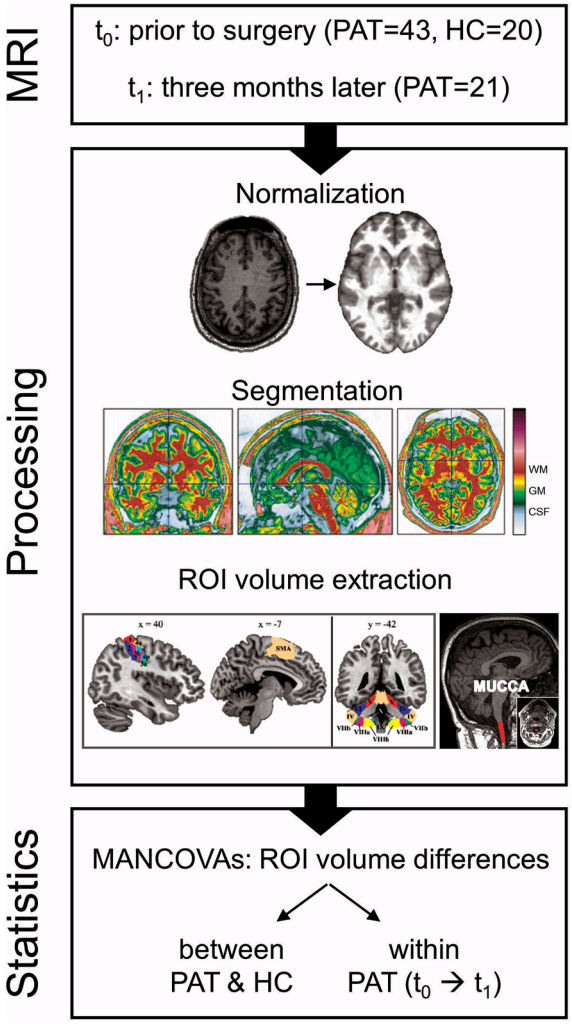

Fig. 2. Flowchart of applied methods.

post-operative (t_2) changes in patients.

2.5. Statistics

All statistical analyses were performed with SPSS 24. Statistical comparisons were tested two-sided with a significance level of $p < .05$, and Bonferroni corrected. In addition, standardized effect sizes (ES) with the respective confidence intervals (CI, Hedges Bias corrected) were computed.

2.6. Demographic and clinical parameters

Initial differences in age, gender and handedness between patients and controls were explored performing independent sample *t*-test and chi-square tests, respectively. Clinical group differences in mJOA and NDI were analyzed using independent sample t-tests.

2.7. Volumetric differences

Initial volumetric group differences were analyzed applying multivariate ANCOVAs, including group (patients, HC) as between-subject factor, ROI volume (GM and WM of MI, SI, and cerebellum, respectively) as dependent variable and ICV as covariate. Volumetric differences in the GM of the SMA were explored using a univariate ANCOVA, including group (patients, HC) as between-subject factor, ROI volume as dependent variable and ICV as covariate.

Differences in cerebral "control" areas were analyzed applying multivariate ANCOVAs, including group (patients, HC) as between-subject factor, control areal volume (GM and WM of the fusiform gyrus and the hippocampus, respectively) as dependent variable and ICV as covariate.

Similarly, to account for an upward progression of atrophy in patients, differences in MUCCA were tested using a univariate ANCOVA, including group (patients, HC) as between-subject factor, MUCCA volume as dependent variable and ICV as covariate. The relationship between MUCCA volume GM, WM, and all ROIs (MI, SI, SMA, CB) was analyzed for patients and HC separately by applying partial correlation analyses, controlling for ICV, and Bonferroni correction for multiple testing ($p = .05/17$ variables, adjusted $p = .003$).

2.8. mJOA subgroup differences

In addition, subgroup differences in ROI volume were analyzed applying multivariate ANCOVAs, including group (mJOAnone-mild, mJOAmoderate, mJOAsevere) as between-subject factor, ROI volume (GM and WM of MI, SI, and cerebellum) as dependent variables and ICV as covariate. Volumetric differences in the GM of the SMA were explored using a univariate ANCOVA, including group (mJOAnone-mild, mJOAmoderate, mJOAsevere) as between-subject factor, ROI volume as dependent variable and ICV as covariate. To exclude a moderating effect of symptom duration, we ensured that the duration of symptoms in subgroups did not differ, as explored by a univariate ANCOVA ($F(2, 34) = 0.174$, $p = .841$.

2.9. Differences during disease progression

To investigate clinical changes during disease progression, patients' mJOA and NDI scores were analyzed using paired samples t-tests. Patients' volumetric alterations in ROI scores from initial to follow-up examination were explored by means of repeated measures ANCOVAs, including ROI volumes as dependent variables and ICV as covariate. Analyses of volumetric changes in subgroups based on symptom severity were not performed because the number of cases in individual subgroups at the post-operative assessment was too small.

2.10. The correlation between volumetric and clinical parameters

The correlation between volumetric and clinical parameters was analyzed in patients using Pearson's partial correlation analyses, controlling for effects of ICV.

3. Results

3.1. Demographic and clinical parameters

Patients and HC did not differ significantly in age, gender or handedness (age: $t(58.50) = 1.09$, $p = .280$; gender: $\chi = 0.35$, $p = .556$; handedness: $\chi = 0.44$, $p = .506$). With regard to clinical measures, patients revealed lower mJOA and higher NDI scores than HC (mJOA: $t(42) = 14.77$, $p = .000$; NDI: $t(51.31) = -9.26$, $p = .000$), see Table 1.

3.2. Volumetric differences

Patients and HC differed significantly in GM SI ($F(4, 57) = 3.33$, $p = .016$), revealing a lower GM volume in area 1, area 2, and area 3b for patients compared to HC (area 1: $F(1, 60) = 9.19$, $p = .004$; area 2: $F(1, 60) = 7.03$, $p = .010$; area 3b: $F(1, 60) = 5.00$, $p = .029$).

Significant group differences were found in GM cerebellar regions ($F(8, 53) = 3.97$, $p = .001$), with lower GM volume in areas IV, V, VIIIa and VIIIb for patients than for HC (area IV: $F(1, 60) = 4.16$, $p = .046$; area V: $F(1, 60) = 6.56$, $p = .013$; area VIIIa: $F(1, 60) = 18.11$, $p = .000$; area VIIIb: $F(1, 60) = 13.08$, $p = .001$).

With regard to "control" areas, multivariate analyses did not reveal significant GM group differences between patients and HC of the of the fusiform gyrus ($F(4, 57) = 1.03$, $p = .397$) or the hippocampus ($F(5, 56) = 1.60$, $p = .176$). Similarly, WM group differences did not reach significance (fusiform gyrus: $F(4, 57) = 0.86$, $p = .497$; hippocampus: $F(5, 56) = 2.16$, $p = .072$).

Significant volume differences in MUCCA were found between patients, indicating lower volumes in patients as compared to HC ($F(1, 60) = 21.07$, $p = .000$). Partial correlation analyses revealed a significant correlation between MUCCA volume and patients' overall WM ($r = 0.36$, $p = .018$), MI (area 4p: $r = 0.35$, $p = .024$), and the CB (area V: $r = 0.31$, $p = .048$). However, none of these significant correlations once subjected to Bonferroni-correction for multiple testing (adjusted $p = .003$). In HC, no significant correlations were found between MUCCA, GM, WM or any ROI.

WM group differences did not reach significance. For detailed results on volumetric differences, see Table 2.

3.3. mJOA subgroup differences

Symptom severity subgroup analyses showed significant differences in GM MI ($F(4, 118) = 5.33$, $p = .001$), both in areas 4a and 4p (area 4a: $F(2, 59) = 8.34$, $p = .001$; area 4p: $F(2, 59) = 6.70$, $p = .002$). Post-hoc tests revealed significantly higher GM volume in area 4a comparing participants with none-mild symptoms to patients with moderate ($p = .014$) or severe symptoms ($p = .001$). In area 4p, the none-mild symptom group had a higher GM volume than the severe symptom group ($p = .002$).

With regard to GM cerebellar volume, significant subgroup differences were found ($F(16, 106) = 1.80$, $p = .040$), specifically regarding areas IV, V, VIIIa, VIIIb and X (area IV: $F(2, 59) = 4.21$, $p = .020$; area V: $F(2, 59) = 4.60$, $p = .014$; area VIIIa: $F(2, 59) = 4.92$, $p = .011$; area VIIIb: $F(2, 59) = 3.38$, $p = .041$; area X: $F(2, 59) = 3.17$, $p = .049$). Post-hoc tests showed a higher GM volume in areas IV and V for participants with none-mild as compared to patients with severe symptoms ($p = .016$ and $p = .011$, respectively). Similar results were found for cerebellar areas VIIIa and VIIIb ($p = .014$ and $p = .045$, respectively).

Subgroups differed significantly in GM SMA ($F(2, 59) = 5.33$, $p = .007$). Post-hoc tests showed significantly higher GM volume for participants with none-mild symptoms as compared to patients with moderate or severe symptoms ($p = .029$ and $p = .022$, respectively).

No WM differences between severity subgroups were evident. For detailed results on subgroup differences, see Fig. 3.

3.4. Differences during disease progression

Patients' clinical status improved significantly after decompression (mJOA: $t(17) = -4.24$, $p = .001$; NDI: $t(17) = 2.63$, $p = .018$). Patients' GM and WM volume did not change significantly (GM: MI ($F(2, 18) = 0.18$, $p < .839$), SI ($F(4, 16) = 0.36$, $p = .832$), CB ($F(8, 12) = 1.87$, $p = .159$), SMA ($F(1, 19) = 0.02$, $p = .900$); WM: MI ($F(2, 18) = 0.68$, $p = .521$), SI ($F(4, 16) = 0.63$, p=.648), CB ($F(8, 12) = 0.99$, $p = .486$)).

3.5. The correlation between volumetric and clinical parameters

Partial correlation analyses revealed a trend towards significant associations between patients' mJOA score and MI, indicating higher mJOA scores to go along with higher GM volume in areas 4a and 4p (mJOA-area4a: $r_{partial} = 0.33$, $p = .054$; mJOA-area4p: $r_{partial} = 0.33$, $p = .058$).

4. Discussion

This study investigated pre- and postoperative structural alterations of the brain as a potential indicator for secondary harm due to chronic cervical cord compression and micro trauma in patients with DCM. Furthermore, disease-related and symptom severity-based volume alterations in GM and WM ROIs were analyzed, as well as their association

Table 1
Clinical differences (mJOA and NDI) between patients and controls.

	PAT (n = 43)		HC (n = 20)					PAT pre-op (n = 21)		PAT post-op (n = 21)				
DV	M	SE	M	SE	p	ES	CI	M	SE	M	SE	p	ES	CI
Age	61	1.70	64	1.40	0.280	−0.03	[−0.84 – 0.23]	59	2.29	–	–	–	–	–
mJOA	11	0.46	18	0.00	**0.000**	−2.78	[-3.50 – −2.06]	11	0.74	13	0.86	**0.001**	−0.55	[−1.22 – 0.11]
NDI	40	3.58	4	1.45	**0.000**	−1.85	[1.22 – 2.47]	49	4.96	35	5.61	**0.018**	0.61	[−0.06 – 1.28]

Note. DV = dependent variables, PAT = patient group, HC = healthy controls, n = number of subjects included, M = mean, p = significance value, SE = standard error, ES = effect size, CI = confidence interval, mJOA = modified Japanese Orthopaedic Association scale, NDI = neck disability index. Group comparisons revealing a significance of $p < .05$ are printed in bold.

Table 2
Volumetric differences between patients and controls.

	PAT (n = 43)		HC (n = 20)					PAT pre-op(n = 21)		PAT post-op (n = 21)				
DV	M	SE	M	SE	p	ES	CI	M	SE	M	SE	p	ES	CI
ICVin cm^3	1413.72	20.16	1479.12	37.78	0.100	−0.44	[−0.98 – 0.09]	1400.87	35.06	1397.43	35.26	0.490	0.02	[−0.58 – 0.63]
GMin cm^3	494.28	5.92	506.10	8.75	0.272	−0.54	[−1.08 – 0.00]	485.00	9.27	484.48	8.46	0.629	0.02	[−0.59 – 0.62]
WMin cm^3	572.31	6.00	607.75	8.87	**0.002**	−0.96	[−1.51 – −0.40]	576.86	6.56	569.43	7.56	0.845	0.14	[−0.46 – 0.75]
MI (4a) in mL	2.39	0.04	2.56	0.06	**0.018**	−0.77	[−1.32 – −0.22]	2.46	0.04	2.43	0.05	0.858	8.11	[6.28 – 9.95]
MI (4p)in mL	0.66	0.02	0.71	0.02	0.110	−0.48	[−1.02 – 0.06]	0.68	0.02	0.67	0.02	0.571	0.12	[−0.49 – 0.72]
SI (1)in mL	0.81	0.01	0.89	0.02	**0.004**	−0.92	[−1.47 – −0.37]	0.83	0.02	0.82	0.03	0.840	0.10	[−0.51 – 0.70]
SI (2)in mL	1.53	0.04	1.70	0.05	**0.010**	−0.75	[−1.30 – −0.20]	1.57	0.05	1.55	0.05	0.075	0.09	[−0.52 – 0.69]
SI (3a)in mL	0.47	0.01	0.51	0.02	0.087	−0.57	[−1.11 – −0.03]	0.47	0.02	0.46	0.01	0.338	0.15	[−0.46 – 0.76]
SI (3b)in mL	1.59	0.03	1.72	0.05	**0.029**	−0.72	[−1.26 – −0.17]	1.64	0.04	1.62	0.05	0.087	0.09	[−0.52 – 0.69]
SMAin mL	5.67	0.09	5.95	0.14	0.092	−0.63	[−1.17 – −0.09]	5.84	0.14	5.80	1.5	0.900	0.05	[−0.55 – 0.66]
CB (IV)in mL	1.74	0.03	1.86	0.05	**0.046**	−0.74	[−1.29 – −0.19]	1.76	0.03	1.73	0.04	0.039	0.13	[−0.74 – 0.47]
CB (V)in mL	1.71	0.04	1.88	0.06	**0.013**	−0.84	[−1.39 – −0.29]	1.71	0.04	1.69	0.04	0.764	0.09	[−0.51 – 0.70]
CB (VI)in mL	1.61	0.03	1.68	0.05	0.235	−0.49	[−1.03 – 0.04]	1.67	0.04	1.65	0.05	0.182	0.07	[−0.53 – 0.68]
CB (VIIb)in mL	2.72	0.05	2.78	0.08	0.488	−0.38	[−0.92 – −15]	2.83	0.07	2.79	0.08	0.163	0.09	[−0.51 – 0.70]
CB (VIIIa)in mL	0.45	0.01	0.53	0.02	**0.000**	−1.21	[−1.78 – −0.64]	0.46	0.02	0.46	0.02	0.641	0.00	[−0.60 – 0.60]
CB (VIIIb)in mL	1.02	0.02	1.16	0.03	**0.001**	−1.05	[−1.61 – −0.49]	1.04	0.04	1.02	0.04	0.017	0.11	[−0.49 – 0.72]
CB (IX)in mL	1.72	0.03	1.80	0.05	0.211	−0.51	[−1.04 – 0.03]	1.76	0.04	1.74	0.05	0.002	0.08	[−0.52 – 0.69]
CB (X)in mL	3.57	0.07	3.68	0.10	0.361	−0.45	[−0.99 – 0.08]	3.67	0.08	3.62	0.08	0.069	0.11	[−0.50 – 0.71]

Note. DV = dependent variables, PAT = patient group, HC = healthy controls, n = number of subjects included, M = mean, p = significance value, SE = standard error, ES = effect size, CI = confidence interval, ICV = intracranial volume, MI = primary motor cortex, SI = primary somatosensory cortex, SMA = supplementary motor cortex, CB = cerebellum. Group comparisons revealing a significance of $p < .05$ are printed in bold.

with clinical status. Results demonstrate initial volume reductions in cerebral and cerebellar regions for patients as compared to controls, supporting the hypothesis of secondary harm to cortical structures in association with chronic compression of the spinal cord. Volumetric alterations appeared to vary depending on symptom severity, revealing GM atrophy not only in patients with severe symptoms but already in those with moderate symptom manifestation. The analysis of GM volume deviations in relevant brain regions related to clinical symptoms of DCM might serve as a potential indicator of ongoing disease progression and should be considered in further patient care and treatment.

The present results revealed significant atrophy in supratentorial GM ROIs of MI and SI for patients, and correspond to previous studies of acute spinal cord injury (Freund et al., 2011; Hou et al., 2014; Wrigley et al., 2009; Jurkiewicz et al., 2007). There are a number of potential reasons for this pathomechanism of indirect brain atrophy arising from spinal cord injury. For example, a retrograde neuronal degeneration from the location of spinal cord injury has been presumed to cause cortical GM loss (Beaud et al., 2008; Hains et al., 2003). In addition, investigating decreased cortical connectivity and reduced angiogenetic activity may help to explain these secondary impairments in the brain (Kim et al., 2006; Fields, 2008). Other research suggested that reduced activity in neural cells, particular in the somatosensory cortex and due to decreased signal transmission, may lead to atrophy in these areas (Jones, 2000). A similar study detected significant GM loss in the sensorimotor cortices and the thalami in their DCM patient's cohort (Bernabéu-Sanz et al., 2020). Even in neurodegenerative diseases like Alzheimer disease, cerebral volume changes are associated with spinal anatomical disorders (Lorenzi et al., 2020). Results are consistent with our findings and uphold the hypothesis of secondary brain impairment due to chronic compression of the cervical spinal cord.

With regard to cerebellar volume alterations, patients revealed GM atrophy in multiple ROIs (areas IV, V, VIIIa, VIIIb). The regions affected are mainly part of the motor cerebellum and connected with sensorimotor areas in the cerebrum (Jones et al., 2013). An impairment of these cerebellar structures can be accompanied by severe clinical dysfunction such as undynamic movement sequences, gait ataxia and reduced fine motoric skills (Zilles and Rehkämper, 1998). In particular, hand representation is located in lobules IV and V, while lobules VIII represent both, hand and leg (Jones et al., 2013). Given the severity of clinical symptoms present in our cohort, atrophy in cerebellar areas as documented here appears plausible. However, results are only partly in line with previous research, demonstrating WM loss throughout the brain, especially in the corticospinal tract (Bernabéu-Sanz et al., 2020) and in cerebellar areas (Freund et al., 2011; Hou et al., 2014). Some studies observed significant WM volume reductions in the cerebellar peduncles in patients with spinal cord injury (Freund et al., 2011; Hou et al., 2014) or found significantly reduced fractional anisotropy in cerebellar peduncles related to DCM as a sign of structural secondary impairment caused by chronic compression of the spinal cord (Bernabéu-Sanz et al., 2020). In contrast, the present results did not reveal WM differences between patients and HC. The discrepancy in results might be due to the selection of ROIs in this study, which focused on brain regions with

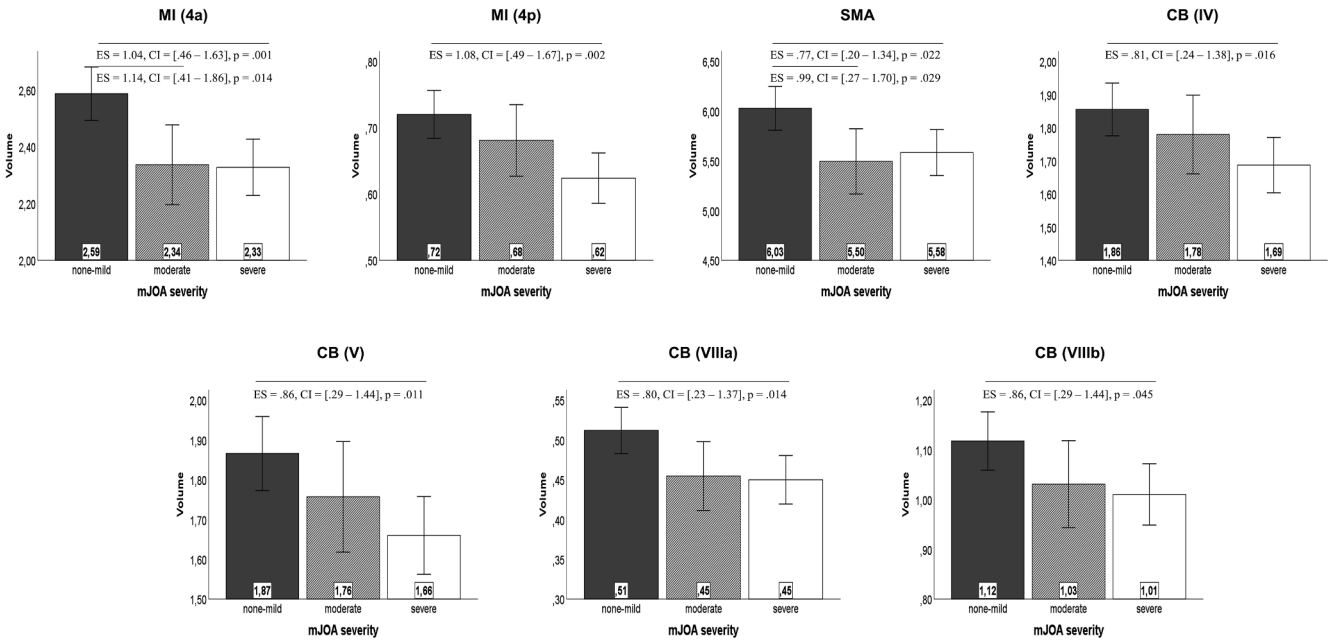

Fig. 3. Significant volumetric differences between mJOA subgroups. Significant volumetric differences in gray matter regions of interest between subgroups are visualized for participants with mild-none (dark grey, n = 27), moderate (lined, n = 12), and severe (white, n = 24) symptoms, including the mean (M). Significances for each analysis were computed two-sided with a significance level of $p < .05$ and corrected for multiple comparisons, including standardized effect sizes (ES) and confidence intervals (CI).

predominant GM clusters rather than on fiber tracts connecting GM ROIs. Nevertheless, the present findings and those of previous studies emphasize secondary cerebellar deterioration arising from spinal cord injury. This is supported by the finding of reduced MUCCA volumes in patients as compared to HC in the present study. This significant loss of volume could be interpreted as a possible upward progression of atrophy in MUCCA, indicating further harm to adjacent spinal cord areas distant to the main areas of stenosis. The association between MUCCA atrophy, clinical disability and disease progression has already been described in the context of multiple sclerosis (Liu et al., 2016). Even in the context of DCM, the degree of (WM) abnormalities in the spinal cord correlates with the clinical status of patients. (Wen et al., 2014; Jones et al., 2013; Rindler et al., 2017; Gao et al., 2013)

Volumetric subgroup differences were present in MI, the SMA, as well as in most cerebellar regions. GM atrophy was prominent especially in patients with severe symptoms as compared to participants with none-mild symptom severity. Moreover, in MI and the SMA, patients with moderate symptoms revealed lower GM volume than the none-mild symptom severity group. Previous studies that investigated patient groups with varying symptom severity primarily focused on the interplay and improvement of different clinical parameters (Kalsi-Ryan et al., 2019), their relevance for post-operative outcome (Chibbaro et al., 2009; Fehlings et al., 2013), or investigated differences in the efficacy of surgery between severity groups (Kopjar et al., 2018). To our knowledge, the present study is the first to show initially present GM volumetric differences related to patients' symptom severity.

In the present study, patients with severe symptoms revealed volume reductions in almost all investigated GM ROIs, further supporting our hypothesis of secondary harm to cortical structures in association with chronic compression of the spinal cord (Wang et al., 2018; Bernabéu-Sanz et al., 2020). In general, surgical intervention has shown to bring significant functional improvements at short- and long-term follow-up (Fehlings et al., 2017). Nevertheless, for patients with mild or moderate DCM, conservative care is often the treatment of choice (Milligan et al., 2019). Considering that significant (and irreversible) GM volume reductions did already manifest in patients with moderate symptoms, it might be worth considering the degree of clinical symptom manifestation in addition to morphologically apparent compromises when deciding whether surgical interventions might be preferable to monitoring disease progression. As the duration of symptoms did not differ between symptom severity subgroups, it is likely that secondary injury (possibly related to chronic spinal cord compression) might occur earlier and faster than the progression of DCM would usually suggest. In that case, the analysis of GM volume deviations in relevant brain regions related to the clinical symptoms of DCM might serve as a potential indicator of ongoing disease progression and should be considered in further patient care and treatment.

Follow-up examinations were performed three months after decompressive surgery. By that time, patients' clinical status had improved significantly, while brain volumetry was unchanged. The absence of volumetric changes after decompression might be due to the relatively short time interval between both measurements. Another reason for the discrepancy between outcome and volumetric response might be a functional reorganization due to GM loss. The effect of cerebral plasticity after acute spinal cord injury and chronic compression of the spinal cord has been described before (Kim et al., 2006; Henderson et al., 2011; Zhou et al., 2015). In addition, compensatory changes in the cortex like reorganized synaptic connectivity and changes in the representational map in sensory brain areas have been reported y (Jain et al., 1997; Pons et al., 1991; Topka et al., 1991). Due to the chronic character of the disease, similar processes might occur in DCM as well, and functional processing in affected brain areas may be reorganized and shifted to different areas during the process of recovery.

4.1. *Limitations and future perspectives*

The small sample size of the control group limited the application of statistical approaches to analyze research questions. Considering the potential variance that might be accompanied by factors such as sex, age, and brain volume, controlling for possible confounding effects by applying regression analyses would be of interest. However, given the small sample size of our study, we tried to account for confounding effects of these factors by matching the patient and control group's mean age and the percentage of men and women included. Furthermore, ICV

was included as covariate in all analyses, controlling for ROI volume differences due to differences in brain sizes between subjects.

In addition, the small sample size of the post-operative cohort limited the interpretability of results and precluded further subanalyses concerning symptom severity, clinical outcome and disease progression. This would be of interest for future studies in order to gain insights into the potential effect and interplay of different disease characteristics (i.e. symptom severity, disease duration, or localization of trauma). Nonetheless, the focus of this study was the analysis of disease-related GM and WM volumetric alterations distant from the actual location of trauma between patients and HC, thereby addressing effects of secondary injury to cortical structures in association with chronic compression to the spinal cord. The present results indicate remote trauma-induced cortical alterations, suggesting an impairment extending from local changes to remote cerebral structures.

5. Conclusion

The present study revealed significant GM volume reductions in sensory and motor cortex areas, as well as in cerebellar structures related to DCM. Clinical improvement after decompression, however, was not mirrored by additional volumetric changes. Chronic injury to the spinal cord might not be limited to local impairment but may also be reflected in remote anatomical changes. The analysis of GM volume deviations in relevant brain regions related to DCM clinical symptoms might serve as a potential indicator of ongoing disease progression and should be considered in patient care and treatment.

CRediT authorship contribution statement

Kerstin Jütten: Conceptualization, Methodology, Formal analysis, Data curation, Writing - original draft, Visualization, Writing - review & editing. **Verena Mainz:** Validation, Formal analysis. **Gerrit Alexander Schubert:** Methodology, Writing - review & editing. **Robin Fabian Gohmann:** Conceptualization, Methodology. **Tobias Schmidt:** Writing - review & editing, Data curation. **Hani Ridwan:** Investigation, Conceptualization, Methodology, Resources. **Hans Clusmann:** Writing - review & editing, Validation. **Christian Andreas Mueller:** Conceptualization, Methodology, Writing - review & editing. **Christian Blume:** Supervision, Conceptualization, Methodology, Writing - original draft, Writing - review & editing, Project administration.

Declaration of Competing Interest

The authors declare that they have no known competing financial interests or personal relationships that could have appeared to influence the work reported in this paper.

Acknowledgements

The authors thank Eleonore Abel and the entire team of technicians at the Department of Neuroradiology for their great support. Special thanks go to participants of the control group, recruited amongst friends, family and colleagues. The authors also thank Iriann Freemantle for her linguistic revision of the manuscript.

Funding

This research did not receive any specific grant from funding agencies in the public, commercial, or not-for-profit sectors.

Data availability statement

The data that support the findings of this study are available on request from the corresponding author. The data are not publicly available due to privacy or ethical restrictions.

References

Aleksanderek, I., McGregor, S.M., Stevens, T.K., Goncalves, S., Bartha, R., Duggal, N., 2017. Cervical spondylotic myelopathy: metabolite changes in the primary motor cortex after surgery. Radiology 282, 817–825.

Beaud, M.L., Schmidlin, E., Wannier, T., et al., 2008. Anti-Nogo-A antibody treatment does not prevent cell body shrinkage in the motor cortex in adult monkeys subjected to unilateral cervical cord lesion. BMC Neurosci 9, 5.

Bernabéu-Sanz, Á., Mollá-Torró, J.V., López-Celada, S., Moreno López, P., Fernández-Jover, E., 2020. MRI evidence of brain atrophy, white matter damage, and functional adaptive changes in patients with cervical spondylosis and prolonged spinal cord compression. Eur Radiol 30, 357–369.

Blume, C., Geiger, M.F., Brandenburg, L.O., et al., 2020. Patients with degenerative cervical myelopathy have signs of blood spinal cord barrier disruption, and its magnitude correlates with myelopathy severity: a prospective comparative cohort study. Eur Spine J. https://doi.org/10.1007/s00586-020-06298-7.

Blume, C., Geiger, M.F., Müller, M., et al., 2021. Decreased angiogenesis as a possible pathomechanism in cervical degenerative myelopathy. Sci. Rep. 11.

Chibbaro, S., Mirone, G., Makiese, O., George, B., 2009. Multilevel oblique corpectomy without fusion in managing cervical myelopathy: long-term outcome and stability evaluation in 268 patients. J Neurosurg Spine 10, 458–465.

Craciunas, S.C., Gorgan, M.R., Ianosi, B., Lee, P., Burris, J., Cirstea, C.M., 2017. Remote motor system metabolic profile and surgery outcome in cervical spondylotic myelopathy. J Neurosurg Spine 26, 668–678.

Dong, Y., Holly, L.T., Albistegui-Dubois, R., et al., 2008. Compensatory cerebral adaptations before and evolving changes after surgical decompression in cervical spondylotic myelopathy. J Neurosurg Spine 9, 538–551.

Duggal, N., Rabin, D., Bartha, R., et al., 2010. Brain reorganization in patients with spinal cord compression evaluated using fMRI. Neurology 74, 1048–1054.

Eickhoff, S.B., Stephan, K.E., Mohlberg, H., et al., 2005. A new SPM toolbox for combining probabilistic cytoarchitectonic maps and functional imaging data. NeuroImage 25, 1325–1335.

Ellingson, B.M., Salamon, N., Holly, L.T., 2015. Advances in MR imaging for cervical spondylotic myelopathy. Eur. Spine J. 24 (Suppl. 2), 197–208.

Fehlings, M.G., Tetreault, L.A., Wilson, J.R., Skelly, A.C., 2013. Cervical spondylotic myelopathy: current state of the art and future directions. Spine (Phila Pa 1976) 38, S1–S8.

Fehlings, M.G., Wilson, J.R., Kopjar, B., et al., 2013. Efficacy and safety of surgical decompression in patients with cervical spondylotic myelopathy: results of the AOSpine North America prospective multi-center study. J. Bone Joint. Surg. Am. 95, 1651–1658.

Fehlings, M.G., Tator, C.H., Linden, R.D., 1989. The relationships among the severity of spinal cord injury, motor and somatosensory evoked potentials and spinal cord blood flow. Electroencephalogr. Clin. Neurophysiol. 74, 241–259.

Fehlings, M.G., Smith, J.S., Kopjar, B., et al., 2012. Perioperative and delayed complications associated with the surgical treatment of cervical spondylotic myelopathy based on 302 patients from the AOSpine North America Cervical Spondylotic Myelopathy Study. J. Neurosurg Spine 16, 425–432.

Fehlings, M.G., Tetreault, L., Nater, A., et al., 2015. Aging of the global population: the changing epidemiology of disease and spinal disorders. Neurosurgery 77 (Suppl 4), S1–S5.

Fehlings, M.G., Tetreault, L.A., Kurpad, S., et al., 2017. Change in functional impairment, disability, and quality of life following operative treatment for degenerative cervical myelopathy: a systematic review and meta-analysis. Global Spine J. 7, 53S–69S.

Fields, R.D., 2008. White matter in learning, cognition and psychiatric disorders. Trends Neurosci. 31, 361–370.

Freund, P., Weiskopf, N., Ward, N.S., et al., 2011. Disability, atrophy and cortical reorganization following spinal cord injury. Brain 134, 1610–1622.

Friston, K.J., Ashburner, J., Kiebel, S.J., Nichols, T.E., Penny, W.D., 2006. Statistical Parametric Mapping: The Analysis of Functional Brain Images, 1st ed. Academic Press.

Gao, S.-J., Yuan, X., Jiang, X.-Y., et al., 2013. Correlation study of 3T-MR-DTI measurements and clinical symptoms of cervical spondylotic myelopathy. Eur. J. Radiol. 82, 1940–1945.

Hains, B.C., Black, J.A., Waxman, S.G., 2003. Primary cortical motor neurons undergo apoptosis after axotomizing spinal cord injury. J. Comp. Neurol. 462, 328–341.

Henderson, L.A., Gustin, S.M., Macey, P.M., Wrigley, P.J., Siddall, P.J., 2011. Functional reorganization of the brain in humans following spinal cord injury: evidence for underlying changes in cortical anatomy. J. Neurosci. 31, 2630–2637.

Hou, J.M., Yan, R.B., Xiang, Z.M., et al., 2014. Brain sensorimotor system atrophy during the early stage of spinal cord injury in humans. Neuroscience 266, 208–215.

Jain, N., Catania, K.C., Kaas, J.H., 1997. Deactivation and reactivation of somatosensory cortex after dorsal spinal cord injury. Nature 386, 495–498.

Jones, E.G., 2000. Cortical and subcortical contributions to activity-dependent plasticity in primate somatosensory cortex. Annu Rev Neurosci 23, 1–37.

Jones, H.R., Burns, T.M., Aminoff, M.J., Pomerory, S.L., 2013. The Netter Collection of Medical Illustrations - Nervous System Part I Brain, 2nd edn. Elsevier, Maryland, MO, USA.

Jones, J.G.A., Cen, S.Y., Lebel, R.M., Hsieh, P.C., Law, M., 2013. Diffusion tensor imaging correlates with the clinical assessment of disease severity in cervical spondylotic myelopathy and predicts outcome following surgery. AJNR Am. J. Neuroradiol. 34, 471–478.

Jurkiewicz, M.T., Mikulis, D.J., McIlroy, W.E., Fehlings, M.G., Verrier, M.C., 2007. Sensorimotor cortical plasticity during recovery following spinal cord injury: a longitudinal fMRI study. Neurorehabil Neural Repair 21, 527–538.

Kalsi-Ryan, S., Clout, J., Rostami, P., Massicotte, E.M., Fehlings, M.G., 2019. Duration of symptoms in the quantification of upper limb disability and impairment for individuals with mild degenerative cervical myelopathy (DCM). PLoS One 14 e0222134.
Karadimas, S.K., Erwin, W.M., Ely, C.G., Dettori, J.R., Fehlings, M.G., 2013. Pathophysiology and natural history of cervical spondylotic myelopathy. Spine (Phila Pa 1976) 38, S21–S36.
Karadimas, S.K., Moon, E.S., Yu, W.R., et al., 2013. A novel experimental model of cervical spondylotic myelopathy (CSM) to facilitate translational research. Neurobiol Dis 54, 43–58.
Karadimas, S.K., Gatzounis, G., Fehlings, M.G., 2015. Pathobiology of cervical spondylotic myelopathy. Eur. Spine J. 24 (Suppl. 2), 132–138.
Kim, B.G., Dai, H.N., McAtee, M., Vicini, S., Bregman, B.S., 2006. Remodeling of synaptic structures in the motor cortex following spinal cord injury. Exp. Neurol. 198, 401–415.
Kopjar, B., Bohm, P.E., Arnold, J.H., Fehlings, M.G., Tetreault, L.A., Arnold, P.M., 2018. Outcomes of Surgical decompression in patients with very severe degenerative cervical myelopathy. Spine (Phila Pa 1976) 43, 1102–1109.
Kowalczyk, I., Duggal, N., Bartha, R., 2012. Proton magnetic resonance spectroscopy of the motor cortex in cervical myelopathy. Brain 135, 461–468.
Liu, Y., Lukas, C., Steenwijk, M.D., et al., 2016. Multicenter validation of mean upper cervical cord area measurements from head 3D T1-weighted MR imaging in patients with multiple sclerosis. AJNR Am. J. Neuroradiol. 37, 749–754.
Lorenzi, R.M., Palesi, F., Castellazzi, G., et al., 2020. Unsuspected involvement of spinal cord in Alzheimer disease. Front Cell Neurosci 14, 6.
Milligan, J., Ryan, K., Fehlings, M., Bauman, C., 2019. Degenerative cervical myelopathy: diagnosis and management in primary care. Can Fam Physician 65, 619–624.
Pons, T., Garraghty, P., Ommaya, A., Kaas, J., Taub, E., Mishkin, M., 1991. Massive cortical reorganization after sensory deafferentation in adult macaques. Science 252, 1857–1860.
Rindler, R.S., Chokshi, F.H., Malcolm, J.G., et al., 2017. Spinal diffusion tensor imaging in evaluation of preoperative and postoperative severity of cervical spondylotic myelopathy: systematic review of literature. World Neurosurg. 99, 150–158.
Shamji, M.F., Ames, C.P., Smith, J.S., Rhee, J.M., Chapman, J.R., Fehlings, M.G., 2013. Myelopathy and spinal deformity: relevance of spinal alignment in planning surgical intervention for degenerative cervical myelopathy. Spine (Phila Pa 1976) 38, S147–S148.
Tan, Y., Zhou, F., Wu, L., et al., 2015. Alteration of regional homogeneity within the sensorimotor network after spinal cord decompression in cervical spondylotic myelopathy: a resting-state fMRI study. Biomed. Res. Int. 2015.
Tetreault, L.A., Karpova, A., Fehlings, M.G., 2015. Predictors of outcome in patients with degenerative cervical spondylotic myelopathy undergoing surgical treatment: results of a systematic review. Eur. Spine J. 24 (Suppl. 2), 236–251.
Tetreault, L., Kopjar, B., Nouri, A., et al., 2017. The modified Japanese Orthopaedic Association scale: establishing criteria for mild, moderate and severe impairment in patients with degenerative cervical myelopathy. Eur. Spine J. 26, 78–84.
Topka, H., Cohen, L.G., Cole, R.A., Hallett, M., 1991. Reorganization of corticospinal pathways following spinal cord injury. Neurology 41, 1276–1283.
Tzourio-Mazoyer, N., Landeau, B., Papathanassiou, D., et al., 2002. Automated Anatomical Labeling of Activations in SPM Using a Macroscopic Anatomical Parcellation of the MNI MRI Single-Subject Brain. NeuroImage 15, 273–289.
Vernon, H., Mior, S., 1991. The Neck Disability Index: a study of reliability and validity. J. Manipulative Physiol. Ther. 14, 409–415.
Wang, L., Yu, B., Li, Q., Qi, F., Guo, Q., 2018. Sensorimotor cortex atrophy in patients with cervical spondylotic myelopathy. Neuroreport 29, 826–832.
Wen, C.Y., Cui, J.L., Liu, H.S., et al., 2014. Is diffusion anisotropy a biomarker for disease severity and surgical prognosis of cervical spondylotic myelopathy? Radiology 270, 197–204.
Wrigley, P.J., Gustin, S.M., Macey, P.M., et al., 2009. Anatomical changes in human motor cortex and motor pathways following complete thoracic spinal cord injury. Cereb Cortex 19, 224–232.
Yonenobu, K., Abumi, K., Nagata, K., Taketomi, E., Ueyama, K., 2001. Interobserver and intraobserver reliability of the Japanese orthopaedic association scoring system for evaluation of cervical compression myelopathy. Spine (Phila Pa 1976) 26, 1890–1894 discussion 1895.
Yushkevich, P.A., Piven, J., Hazlett, H.C., et al., 2006. User-guided 3D active contour segmentation of anatomical structures: significantly improved efficiency and reliability. NeuroImage 31, 1116–1128.
Zhou, F.Q., Tan, Y.M., Wu, L., Zhuang, Y., He, L.C., Gong, H.H., 2015. Intrinsic functional plasticity of the sensory-motor network in patients with cervical spondylotic myelopathy. Sci Rep 5, 9975.
Zilles, K., Rehkämper, G., 1998. Funktionelle Neuroanatomie - Lehrbuch und Atlas, 3rd ed. Springer, Berlin Heidelberg.